

ORIGINAL ARTICLE

Open Access



# Experimental Quantification on the Residual Seismic Capacity of Damaged RC Column Members

Chien-Kuo Chiu\*, Hsin-Fang Sung, Kai-Ning Chi and Fu-Pei Hsiao

## Abstract

To quantify the post-earthquake residual seismic capacity of reinforced concrete (RC) column members, experimental data for 6 column specimens with flexural, flexural–shear and shear failure modes are used to derive residual seismic capacity of damaged RC column members for specified damage states in this work. Besides of the experiment data, some related researches are also investigated to suggest the reduction factors of strength, stiffness and energy dissipation capacity for damaged RC column members, respectively. According to the damage states of RC columns, their corresponding seismic reduction factors are suggested herein. Taking an RC column with the flexural–shear failure for an example, its reductions factors of strength, stiffness and energy dissipation capacity are 0.5, 0.6 and 0.1, respectively. This work also proposes the seismic performance assessment method for the residual seismic performance of earthquake-damaged RC buildings. In the case study, this work selects one actual earthquake-damaged school building to demonstrate the post-earthquake assessment of seismic performance for a damaged RC building.

**Keywords:** reinforced concrete, building, residual seismic performance, crack width, reduction factor

## 1 Introduction

In Taiwan, concrete structures damaged by earthquakes are identified with a yellow or red tag after inspection, warning those who will enter the building or prohibiting entry, respectively. After a building is identified as damaged, the owner or user must repair, retrofit, or dismantle it within a specified period. Additionally, the danger tag can only be removed after a government inspection deems the structure safe. Unless a building is completely damaged or collapsed, or unless its drift ratio exceeds collapse criteria, engineers may have difficulty determining whether a building should be retrofitted or demolished without a detailed financial loss estimation. On the basis of investigations made after several major earthquakes occurred in Taiwan, e.g., Ruei-Li earthquake (July 17, 1998), Chi-Chi earthquake (September

21, 1999), and Chia-Yi earthquake (October 22, 1999), a number of low-rise buildings suffered damages of various degrees. Especially in Chi-Chi earthquake, nearly half of the school buildings, which are almost categorized into low-rise reinforced concrete (RC) buildings (building height is lower than 15 m), in the central area of Taiwan collapsed or were damaged seriously. Even in Taipei City, which is about 150 km far away from the epicenter, there were 67 school buildings damaged were damaged in Chi-Chi earthquake. Additionally, school buildings are usually required to act as emergency shelters soon after a disastrous earthquake event. Therefore, a post-earthquake emergent assessment procedure for decision-making for earthquake-damaged buildings is needed.

Many seismic assessment methods for buildings have been developed in recent years (ATC 1996; FEMA 1998, 2000); however, those methods seldom mention re-evaluating the seismic residual of earthquake-damaged buildings. Di Ludovico et al. (2013) proposed the experiment-based expressions of modification factors for stiffness, strength and displacement capacity as a function of the rotational ductility demand. Additionally, the

\*Correspondence: ckchiu@mail.ntust.edu.tw

Department of Civil and Construction Engineering, National Taiwan University of Science and Technology, No. 43, Keelung Rd., Sec.4 Da'an Dist., Taipei City 10607, Taiwan, ROC

Journal information: ISSN 1976-0485 / eISSN 2234-1315

**Table 1 Definition of damage levels of structural members (JBDPA 2001).**

Damage level	Description of damage
I (Slight)	Visible narrow cracks on concrete surfaces. Crack widths are less than 0.2 mm
II (Light)	Visible cracks on concrete surface. Crack widths in the range 0.2 mm–1 mm
III (Moderate)	Localized crushing of concrete cover. Noticeable wide cracks. Crack widths in the range 1–2 mm
IV (Severe)	Crushing of concrete with exposed reinforcing bars. Spalling off of cover concrete. Crack widths are greater than 2 mm
V (Total damage or collapse)	Buckling of reinforcing bars. Cracks in core concrete. Visible vertical deformation in columns, walls, or both. Visible settlement, tilting of the building, or both

proposed expressions can be introduced to modify the moment-rotation plastic hinges of RC columns in the buildings of Mediterranean regions with design characteristics non-conforming to present-day seismic provisions. However, how to apply the modification factors for stiffness, strength and displacement capacity in the seismic performance assessment is not mentioned clearly in the paper. The guidelines developed by JBDPA (2001, 2015) for evaluating the residual seismic performance of earthquake-damaged buildings can be used to determine the damage class of a building; however, the procedure is only suitable for the preliminary seismic performance assessment. Restated, a preliminary seismic performance assessment does not provide sufficient data for engineers or users to make decisions on earthquake-damaged buildings. Additionally, for the detailed seismic performance assessment of low-rise RC building structures in Taiwan, engineers need to use the nonlinear static analysis method, which is different with the method proposed in the JBDPA guidelines (2001, 2015). Therefore, a post-earthquake detailed assessment method of seismic performance is needed to evaluate the residual seismic performance of an earthquake-damaged RC building for the post-earthquake maintenance strategy.

In the JBDPA guidelines (2001, 2015), the reduction factors are suggested using limited experimental data. For the practical use in Taiwan, these reduction factors should be verified using more reliable experimental data. This work uses experimental data for 6 column specimens with various failure modes to derive reduction factors of seismic capacity for specified damage states described in the JBDPA guidelines (2001, 2015) (Table 1). While the reduction factors of seismic capacity are defined using the residual capacity of energy dissipation under cyclic loading, the reduction factors of strength and stiffness are conducted for each RC column specimen. This work also proposes a method that can be used to define nonlinear plastic hinges for damaged RC column members according their damage states and corresponding reduction factors of seismic capacity. Additionally, on the basis of the seismic performance assessment method developed by the NCREC (2009), a post-earthquake detailed

assessment method of seismic performance is developed in this work.

## 2 Quantification of Seismic Damage to RC Column Members

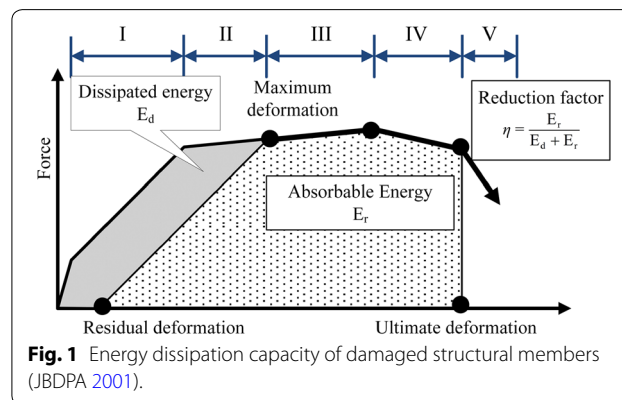
### 2.1 Definition of Reduction Factors of Seismic Capacity

Figure 1 defines the reduction factor  $\eta$  in terms of the dissipated energy  $E_d$  and the residual energy dissipation capacity  $E_r$ . Table 2 presents the reduction factors of seismic capacity related to various RC vertical components that are provided in the Japanese guidelines (JBDPA 2001, 2015). For a column member with the flexural–shear failure, JBDPA (2015) added its corresponding reduction factors of seismic capacity excluded in JBDPA (2001).

$$\eta = \frac{E_r}{E_d + E_r} \tag{1}$$

### 2.2 Reduction Factors of Seismic Capacity of Damaged RC Columns

In place of the reduction factors that are defined in terms of the energy dissipation capacity, Ito et al. (2015) proposed reduction factors of the strength, deformation, and damping ratio of damaged RC column members for evaluating post-earthquake residual seismic performance. The reduction factors of strength were obtained directly from experimental results. For each



**Table 2 Seismic reduction factors suggested by the references (JBDPA 2001, 2015).**

Damage level	RC column			RC wall		RC beam	
	Shear	Flexural–shear	Flexure	Shear	Flexure	Shear	Flexure
I	0.95	0.95	0.95	0.95	0.95	0.95	0.95
II	0.6	0.7	0.75	0.6	0.7	0.7	0.75
III	0.3	0.4	0.5	0.3	0.4	0.4	0.5
IV	0	0.1	0.2	0	0.1	0.1	0.2
V	0	0	0	0	0	0	0

**Table 3 Reduction factors of strength, deformation and damping ratio (Ito et al. 2015).**

Damage level	Flexural member			Shear member			
	$\eta_s$	$\eta_d$	$\eta_h$	$\eta_s$	$\eta_d$	$\eta_h$	$\eta_h$
I	1	1	0.95	1	1	0.9	0.9
II	1	0.95	0.8	1	0.85	0.7	0.7
III	1	0.85	0.75	1	0.75	0.6	0.6
IV	0.6	0.75	0.7	0.4	0.7	0.5	0.5
V	0	0	0	0	0	0	0

$\eta_s$  is the reduction factor of strength;  $\eta_d$  is the reduction factor of deformation;  $\eta_h$  is the reduction of damping ratio.

selected specimen, Ito et al. (2015) used the damage index model of Park and Ang (1985) to estimate the equivalent ultimate deformation capacity; then, the reduction factors of deformation were calculated from the equivalent ultimate deformation capacity. To evaluate the reduction factor of the damping ratio, Ito et al. (2015) used the equivalent damping ratio to quantify the energy dissipation capacity of damaged RC column members, which was studied using the hysteretic energy under cyclic loading. In the post-earthquake assessment of seismic performance of Ito et al. (2015), their nonlinear statistical analysis considered reduction factors of the strength, deformation and damping ratio of flexural and shear members (Table 3).

Poegoeh (2012) utilized experimental data about full-size RC column specimens with various failure modes to study the accuracy of the seismic reduction factors that were suggested by the JBDPA (2001). Poegoeh (2012) acquired experimental data for 16 columns from the NCREE and Japan Society of Civil Engineers (JSCE). Reduction factors of seismic capacity of RC column specimens with various failure modes were analyzed; their failure modes were flexural failure, flexural–shear failure, and shear failure. Based on the application of the residual crack-deformation model in Sect. 2.3, residual deformation data were used to calculate corresponding maximum residual crack widths at various residual drift ratios.

According to the descriptions of damage levels of each RC column specimen (Table 1), the maximum

**Table 4 Suggested reduction factors of seismic capacity for damaged RC columns.**

Damage level	Flexural failure	Flexural–shear failure	Shear failure
I	0.9	0.9	0.9
II	0.7	0.6	0.6
III	0.5	0.3	0.3
IV	0.1	0.1	0
V	0	0	0

residual crack widths were used to classify damage levels to estimate their corresponding reduction factors of seismic capacity. The shear failure of columns adversely affects the safety of any structure. Therefore, residual factors for RC columns with shear failure should be evaluated conservatively. Poegoeh (2012) suggested reduction factors of seismic capacity for damaged RC columns with various failure modes including the flexural–shear mode, which are presented in Table 4.

However, some of the specimens used in Poegoeh (2012) were designed with high-strength materials, including concrete and steel. Moreover, since the maximum residual crack widths were not obtained directly from experimental results, the relationship between the maximum residual crack widths and the reduction factors was not reliably obtained. Therefore, this work considers full-size RC column specimens to confirm

reduction factors of strength, stiffness and energy dissipation capacity. The specimens in this work are designed based on column members that are typically used in low-rise RC buildings in Taiwan.

### 2.3 Relationship Between Residual Crack Width and Residual Deformation

Since the damage level is defined primarily in terms of the residual crack width, the quantification of the relationship between the residual deformation and residual crack width is necessary for the post-earthquake assessment of seismic performance. The residual deformation of a column or beam member is a function of residual flexural crack widths, residual shear crack widths, bond slip of the main bars and the pullout displacement of the main bars from the beam-column joint. According to the Japanese guideline (AIJ 2004), the latter two contributions are negligible. Therefore, the relationship between the residual deformation and residual crack widths can be simplified as Eq. (2) (AIJ 2004). This work focuses only on deformation that is caused by shear and flexural cracking.

$$R = R_f + R_s \tag{2}$$

Figure 2 plots the geometric relationship between residual flexural cracks width and residual deformation. Residual flexural crack widths in the two ends of a member are summed to  $\sum W_f$ ; the residual deformation can then be estimated from the geometric deformation. For convenience, a ratio  $n_f$  of the residual maximum flexural crack width  $W_{f,max}$  to the residual total flexural crack widths  $\sum W_f$  is defined here to estimate the deformation that is caused by the residual flexural cracks (Eq. 3). Experimental results indicate that the ratio  $n_f$  of a beam member with RC of normal strength is approximately 2.0.

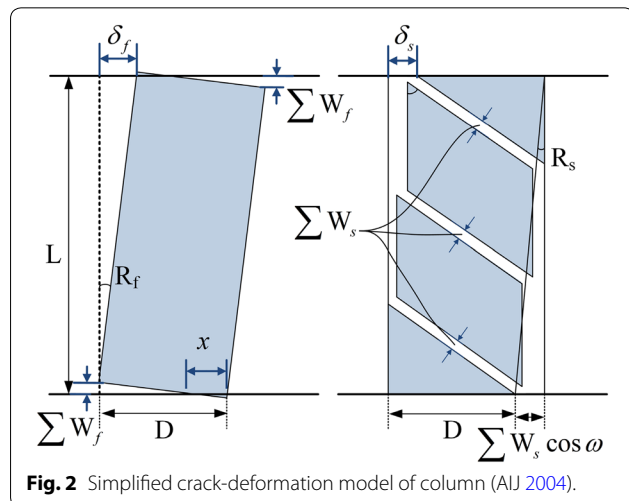


Fig. 2 Simplified crack-deformation model of column (AIJ 2004).

$$R_f = \frac{\sum W_f}{D - x_n} = \frac{n_f \times W_{f,max}}{D - x_n} \tag{3}$$

$$R_s = 2 \times \frac{\sum W_s \times \cos\omega}{L} = 2 \times \frac{n_s \times W_{s,max} \times \cos\omega}{L} \tag{4}$$

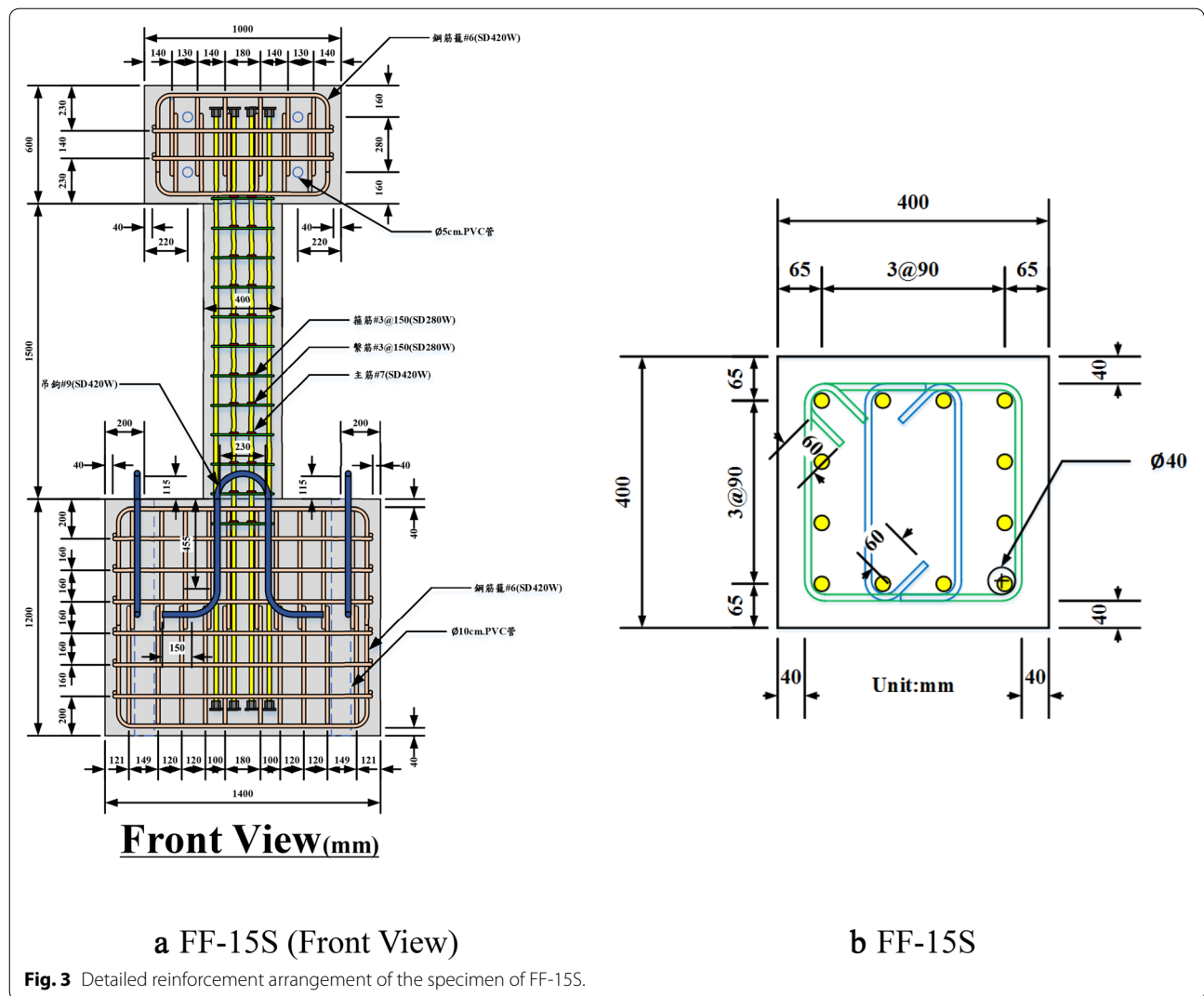
where  $R_f$  is the residual flexural deformation of a column (mm);  $R_s$  is the residual shear deformation of a column (mm);  $W_{s,max}$  is the maximum residual shear crack width of a column (measured) (mm);  $W_{f,max}$  is the maximum residual flexural crack width of a column (measured) (mm);  $\omega$  is the angle between the shear crack and the vertical direction of column (45° is assumed herein);  $n_s$  is the ratio of total width of the residual shear crack to the maximum residual shear crack width ( $\sum W_s/W_{s,max}$ );  $n_f$  is the ratio of total width of the residual flexural crack to the maximum residual flexural crack width ( $\sum W_f/W_{f,max}$ );  $D$  is the column depth (mm);  $L$  is the column clear height (mm); and  $x_n$  is the distance from outermost compression fiber to the neutral axis (0.2D is assumed herein) (mm).

The relationship between the residual shear crack widths and residual deformation can be derived using the concept that was applied to the flexural crack (Fig. 2). However, according to Sugi et al. (2007), the equation derived based on Fig. 2 in AIJ (2004) would overestimate the calculated residual deformation from the residual shear crack. Therefore, Sugi et al. (2007) recommended Eq. (4) that can be used to describe the relationship between the residual shear crack widths and residual deformation. In Eq. (4), residual deformation induced by the residual shear crack can be estimated from the ratio  $n_s$  of the residual maximum shear crack width  $W_{s,max}$  to the residual total shear crack widths  $\sum W_s$  and the residual maximum shear crack width  $W_{s,max}$ . Experimental results indicate that the ratio  $n_s$  of beam members with normal-strength RC is approximately 3–4. However, whether it is applicable to a column member warrants further study. Therefore, this work investigates the relationship between the residual deformation and the residual crack width by conducting an experiment on full-size column specimens with various failure modes.

## 3 Experimental Set-up and Results

### 3.1 Experimental Set-up

The column specimens with single curvature herein are 1800 mm long and their cross-sections are 400 mm × 400 mm, as shown in Fig. 3. Figures 4 and 5a show the loading system for the column specimens with single curvature in this work. Since the experimental set-up cannot let the applied axial loading constant in the experiment, the experimental results cannot be used to investigate the effect of the axial loading on the



reduction factors. For the target building of this work is set to be the low-rise RC buildings, the variation of the axial loading of a column member under earthquake is not significant and constant under earthquake. Therefore, the reduction factors obtained from the experimental set-up in this work can still be used for the low-rise RC buildings. The main bars are SD420 of D22, while the stirrups are SD280 of D10. These specimens have the same tensile reinforcement ratio. Three stirrup ratios are utilized to study the seismic reduction factors of the column specimens with various failure modes, which are flexural failure, flexural–shear failure and shear failure. Two arrangements of the reinforcements in the specimen section is designed and used in this work, as shown in Fig. 3. The measured compressive strength of concrete is approximately 30–37 MPa. Table 5 presents detailed information about each specimen.

To measure crack development, each specimen is brushed with white cement paint and 100 × 100 mm grid lines are drawn on it before testing. The stirrup position is indicated on each specimen. The crack widths are measured under a microscope with a measurement resolution of 0.01 mm. The maximum crack width at a specified peak deformation and the residual crack width with the applied loading set back to zero at each measurement point are recorded in the experiment. The methods for measuring cracks of various types in various positions are as follows (Fig. 6).

1. Flexural crack: cracking occurs where the bending moment stress of a cross section is at its maximum.
2. Shear crack: cracking occurs where the shear stress of a cross section is at its maximum. The width at the intersection between the shear crack and the stirrup,

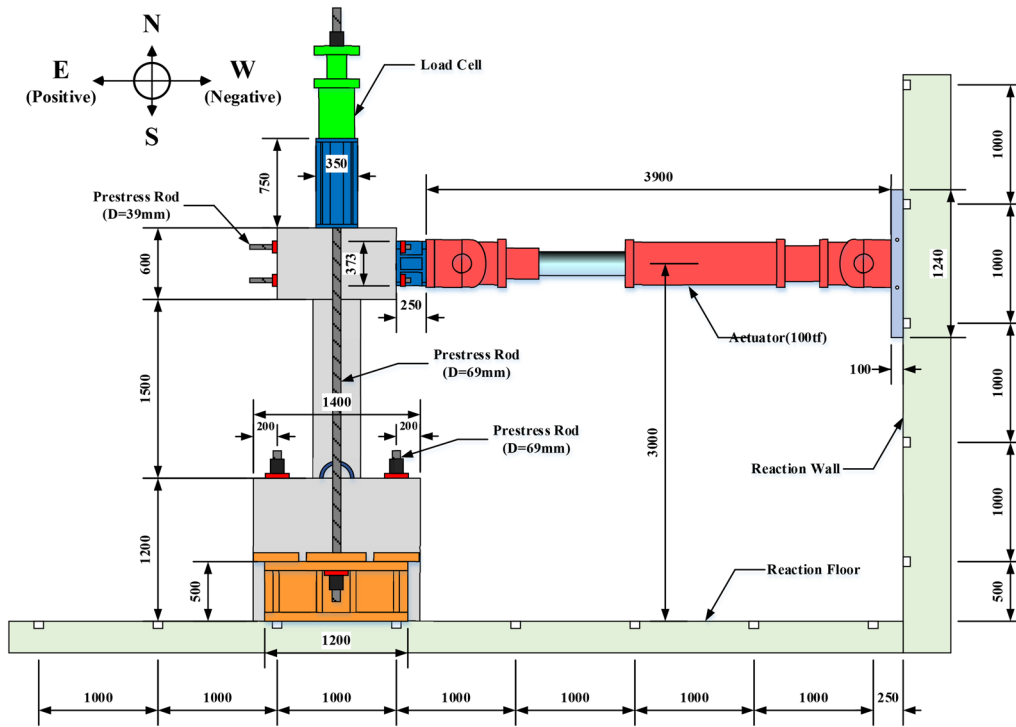
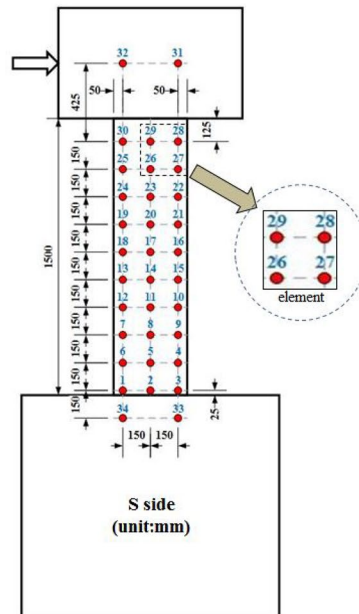


**Fig. 4** Applied loading system for the cantilever beam specimens in this work.



**a** Specimen set-up



**b** Markers of the optical measure system

**Fig. 5** Column specimens with the single curvature.

**Table 5 Detailed information of each specimen.**

Specimen	Failure mode	L (mm)	Cross section (mm <sup>2</sup> )	Concrete cover (mm)	$f'_c$ (MPa)	$f_y$ (MPa)	$f_{yt}$ (MPa)	S (mm)	$\rho_{sh}$ (%)	Axial force
FF-15S	Flexural failure	1800	400 × 400	40	21 (37.0) <sup>a</sup>	420	280	150	0.61	0.1Agf <sub>c</sub> '
	Flexural failure	1800	400 × 400	40	21 (33.1) <sup>a</sup>	420	280	150	0.61	0.2Agf <sub>c</sub> '
FSF-15S	Flexural–shear failure	1800	400 × 400	40	21 (34.6) <sup>a</sup>	420	280	150	0.31	0.1Agf <sub>c</sub> '
	Flexural–shear failure	1800	400 × 400	40	21 (30.8) <sup>a</sup>	420	280	150	0.31	0.2Agf <sub>c</sub> '
SF-30S	Shear failure	1800	400 × 400	40	21 (34.1) <sup>a</sup>	420	280	300	0.15	0.1Agf <sub>c</sub> '
	Shear failure	1800	400 × 400	40	21 (33.2) <sup>a</sup>	420	280	300	0.15	0.2Agf <sub>c</sub> '

<sup>a</sup> The measured compressive strength of concrete at the testing time.

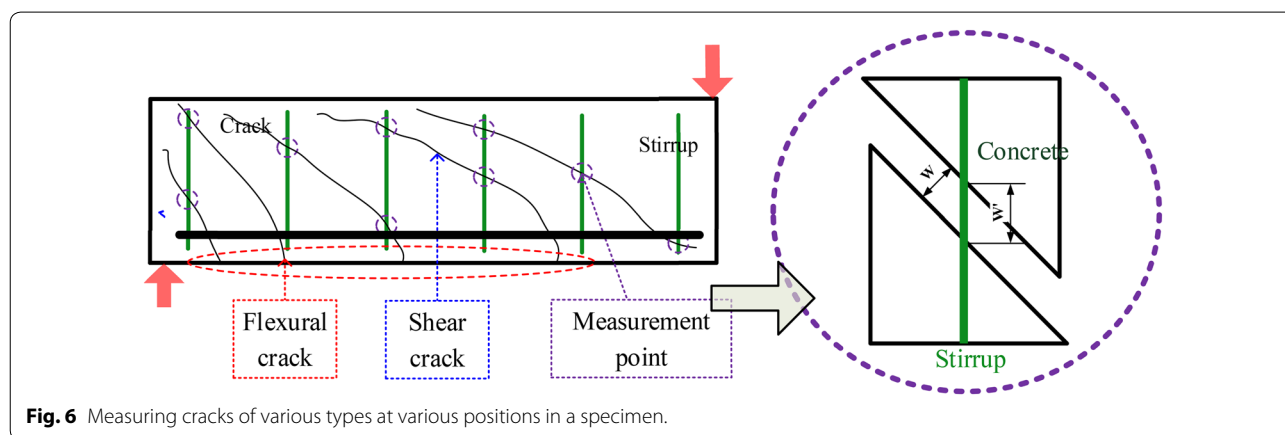


**Fig. 6** Measuring cracks of various types at various positions in a specimen.

which includes the shear crack width and the width parallel to the stirrup, is measured.

The total, flexural, and shear deformation of a specimen can be calculated using the three-dimensional coordinate values that are measured from an optical measurement system, as in Fig. 5b. The total deformation can be evaluated from the amount of change in distance between the markers on the top end of a specimen. The shear deformation of each element, which is constructed by four markers, can be calculated from the amount of change in the diagonal distance; then, the shear deformation of a specimen can be evaluated based on the shear deformation of each element. Additionally, the flexural deformation of a specimen is assumed to be its total deformation minus shear deformation.

### 3.2 Experimental Results

Figure 7 plots the relationship between the lateral force and deformation of each specimen obtained using the applied loading system in Sect. 3.1. To study the damage state, when a specimen is set back to zero deformation from a specified peak drift ratio, the residual crack width is obtained. Figure 8 plots the relationship between the

maximum residual crack width and the peak drift ratio for each specimen. Clearly, except for the specimen of SF-30-0.2, since the residual flexural crack width exceeds the residual shear crack width, the damage levels of I–III for each specimen can be determined using the residual flexural crack width. Additionally, the envelop line of the hysteretic loop for each specimen is used to determine the ultimate deformation point corresponding to the lateral force equal to  $0.8 V_{max}$ .

By visual inspection and applying strain gauges to the reinforcement, peak drift ratios at the initial crack points, at the initial yielding points of the main bars and the stirrup, at maximum loading points, at the compressive concrete spalling points and in the final step for each specimen under cycling loading are obtained and listed in Table 6. Figures 9, 10, 11 show the damage situation of each specimen in the final step.

### 3.3 Relationship Between Crack Width and Deformation of an RC Column Member

According to results obtained using the measurement system that is described in Sect. 3.1, the deformation of each specimen is divided into shear deformation and flexural deformation. In Fig. 12a, for the specimens at

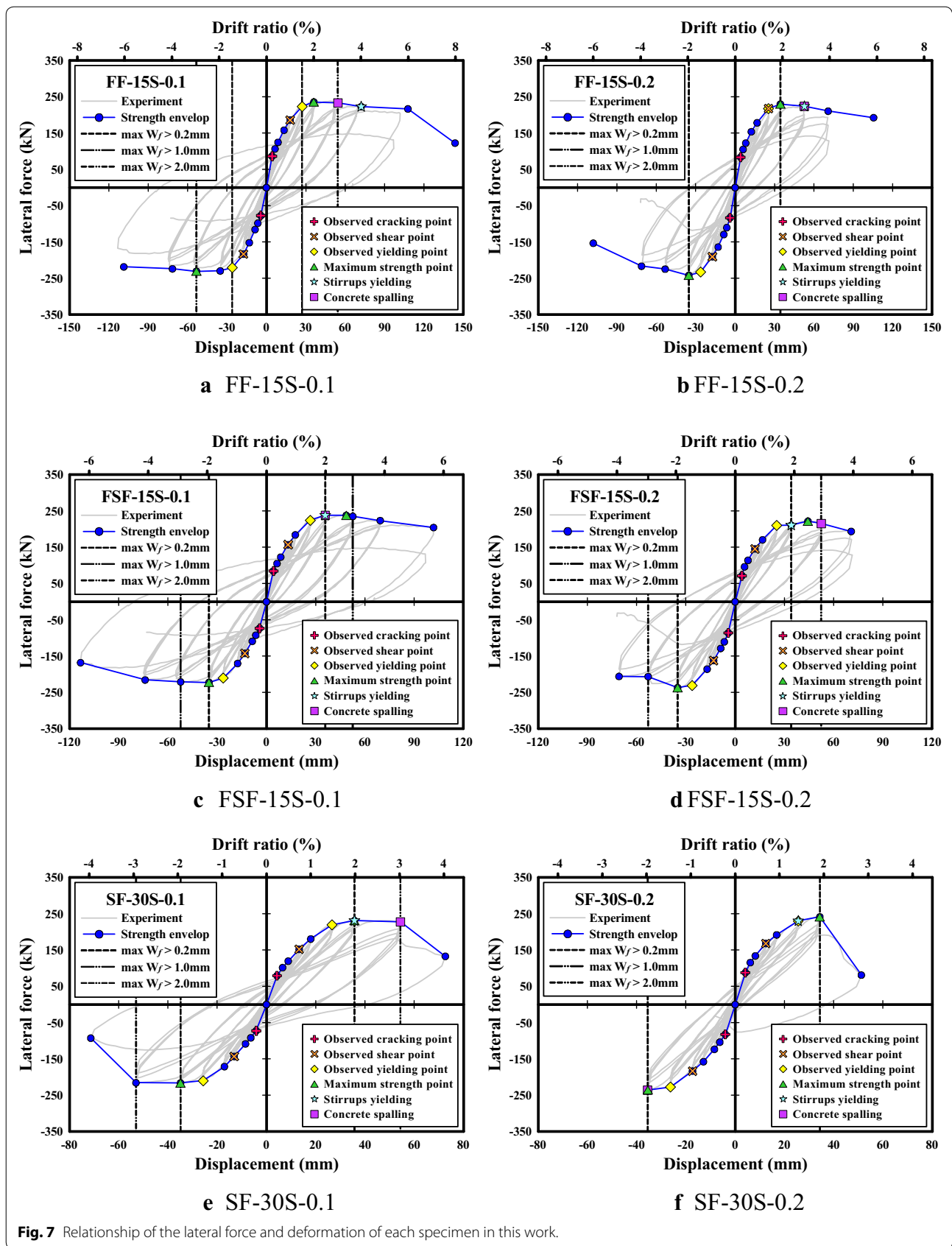


**Fig. 7** Relationship of the lateral force and deformation of each specimen in this work.

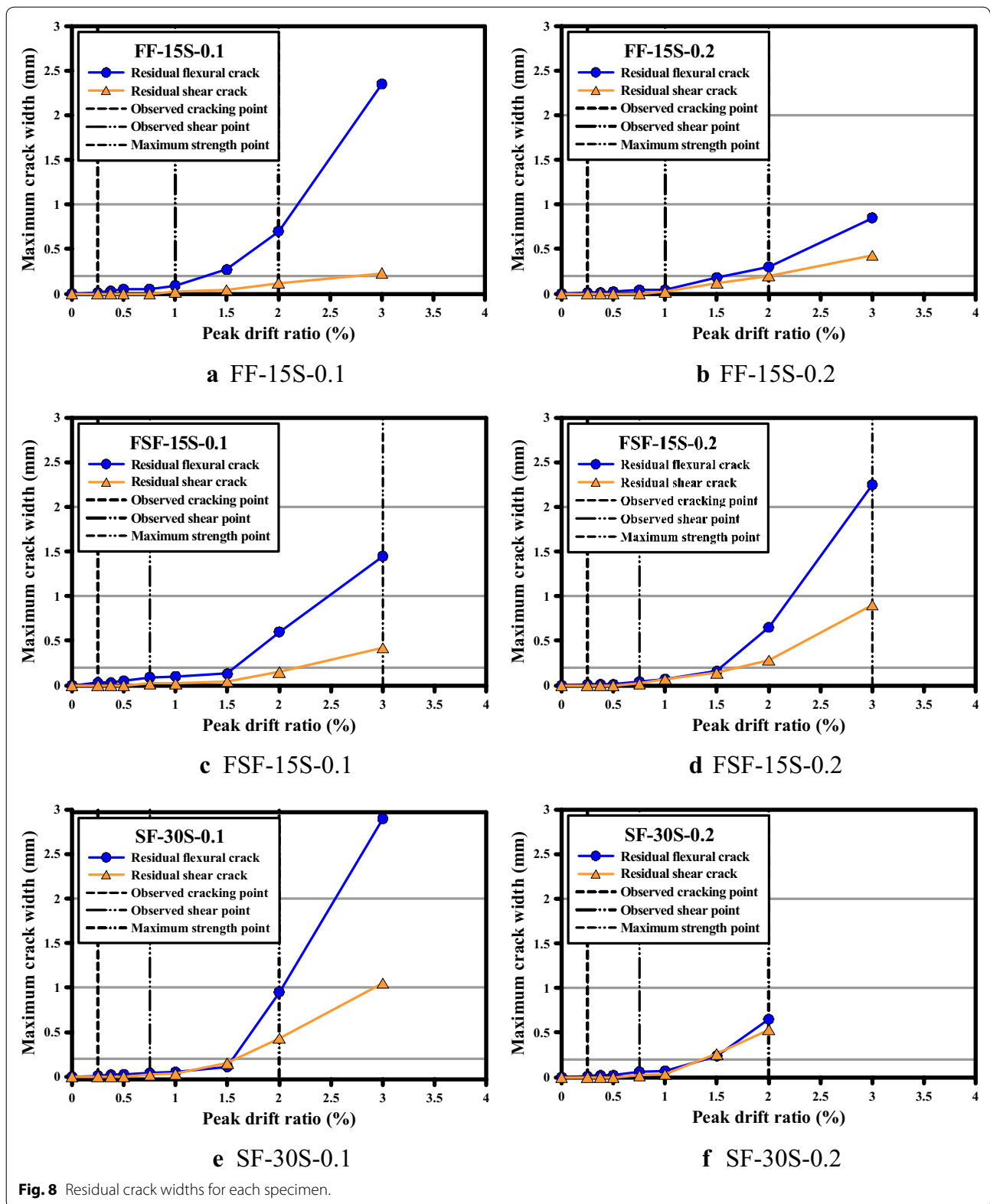
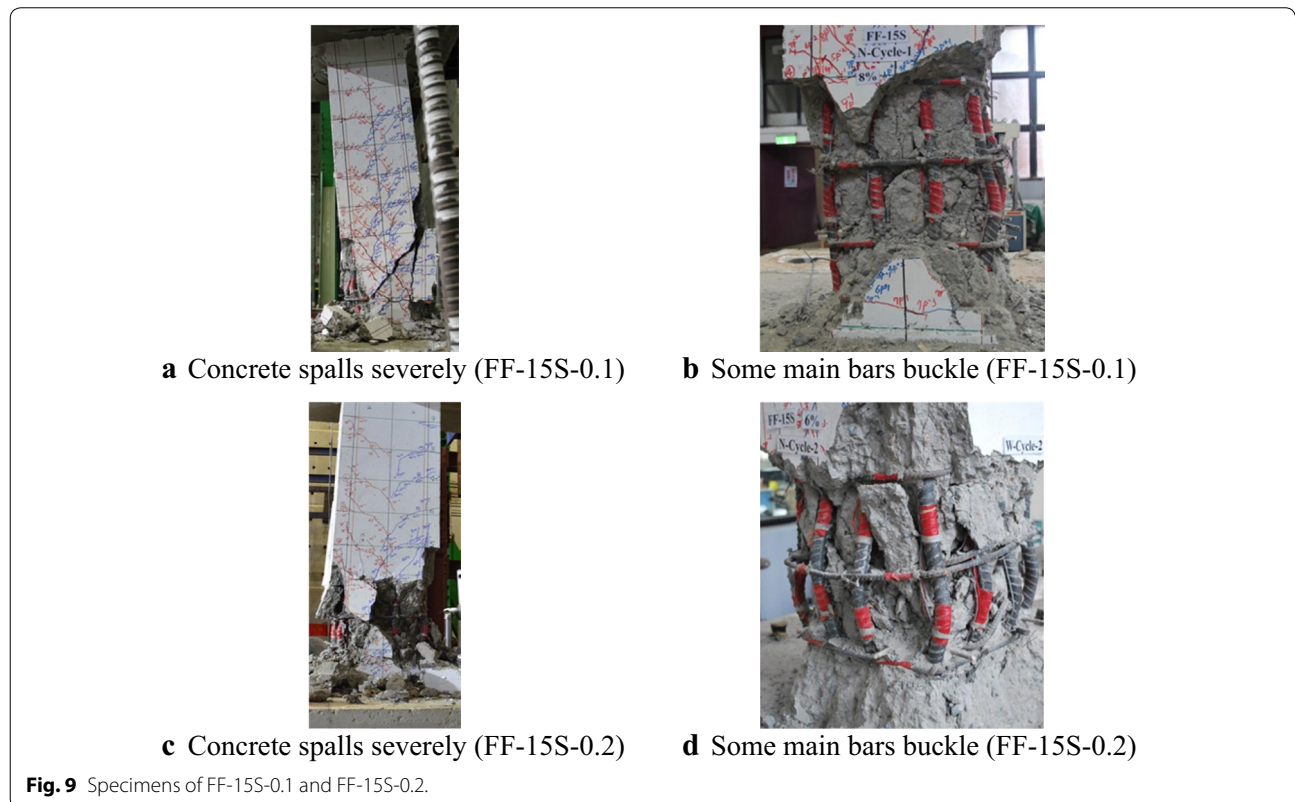


**Table 6 Performance points of each specimen under cyclic loading.**

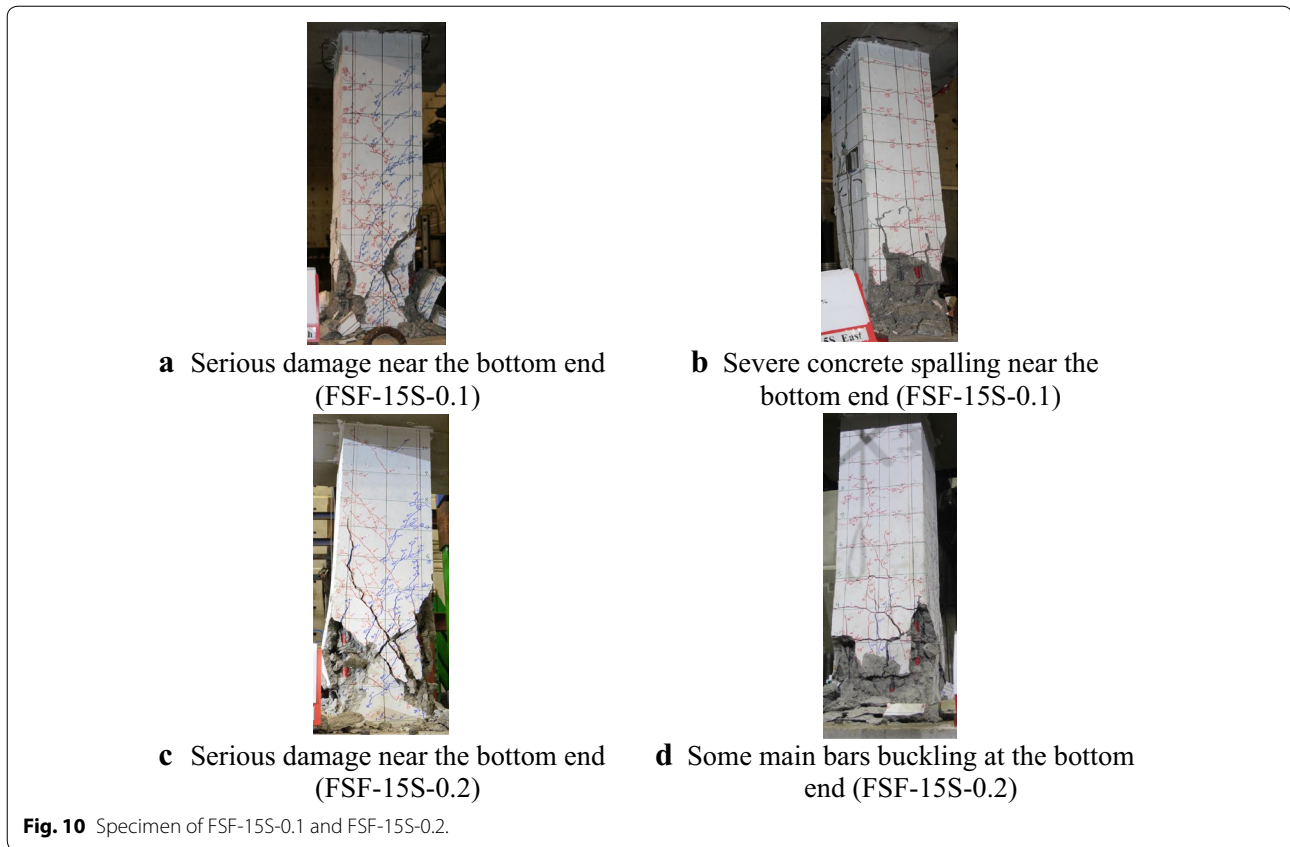
Specimen	Initial flexural crack	Initial shear crack	Initial yielding of main bars	Initial yielding of stirrup	Maximum forward loading	Maximum reverse loading	Concrete spalls	Final step (strength < 60%)
FF-15S-0.1	± 0.25% (1st)	1% (1st)	1.5% (1st)	4% (3rd)	2% (1st)	− 3% (1st)	− 3% (1st)	8% (1st)
FF-15S-0.2	± 0.25% (1st)	− 1% (1st)	1.5% (1st)	3% (1st)	2% (1st)	− 2% (1st)	3% (1st)	6% (2nd)
FSF-15S-0.1	± 0.25% (1st)	0.75% (1st)	1.5% (1st)	2% (3rd)	3% (1st)	− 2% (1st)	− 2% (1st)	6% (2nd)
FSF-15S-0.2	± 0.25% (1st)	0.75% (1st)	1.5% (1st)	2% (3rd)	− 2% (1st)	3% (1st)	3% (1st)	4% (3rd)
SF-30S-0.1	± 0.25% (1st)	0.75% (1st)	1.5% (1st)	± 2% (1st)	2% (1st)	− 2% (1st)	3% (1st)	− 4% (1st)
SF-30S-0.2	± 0.25% (1st)	0.75% (1st)	1.5% (1st)	1.5% (1st)	2% (1st)	− 2% (1st)	2% (1st)	3% (1st)



the peak drift ratio, the flexural deformation is approximately 0.88 of the total deformation. When the applied force of the specimens is set back to zero, the flexural deformation is approximately 0.81 of the total deformation, as shown in Fig. 12b. Regardless of the peak drift ratio or the residual drift ratio, the total deformation

of a specimen can be estimated well using the flexural deformation.

This work investigates the relationship between the residual total crack widths and the residual maximum width of an RC column member based on experimental data. Notably, this relationship can be used to estimate the residual maximum crack width and assess the



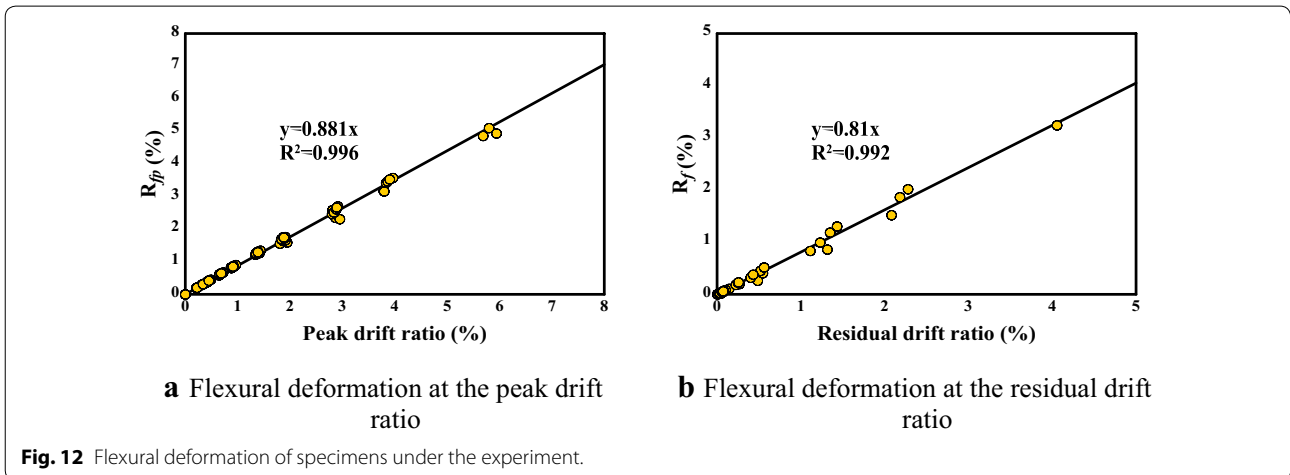
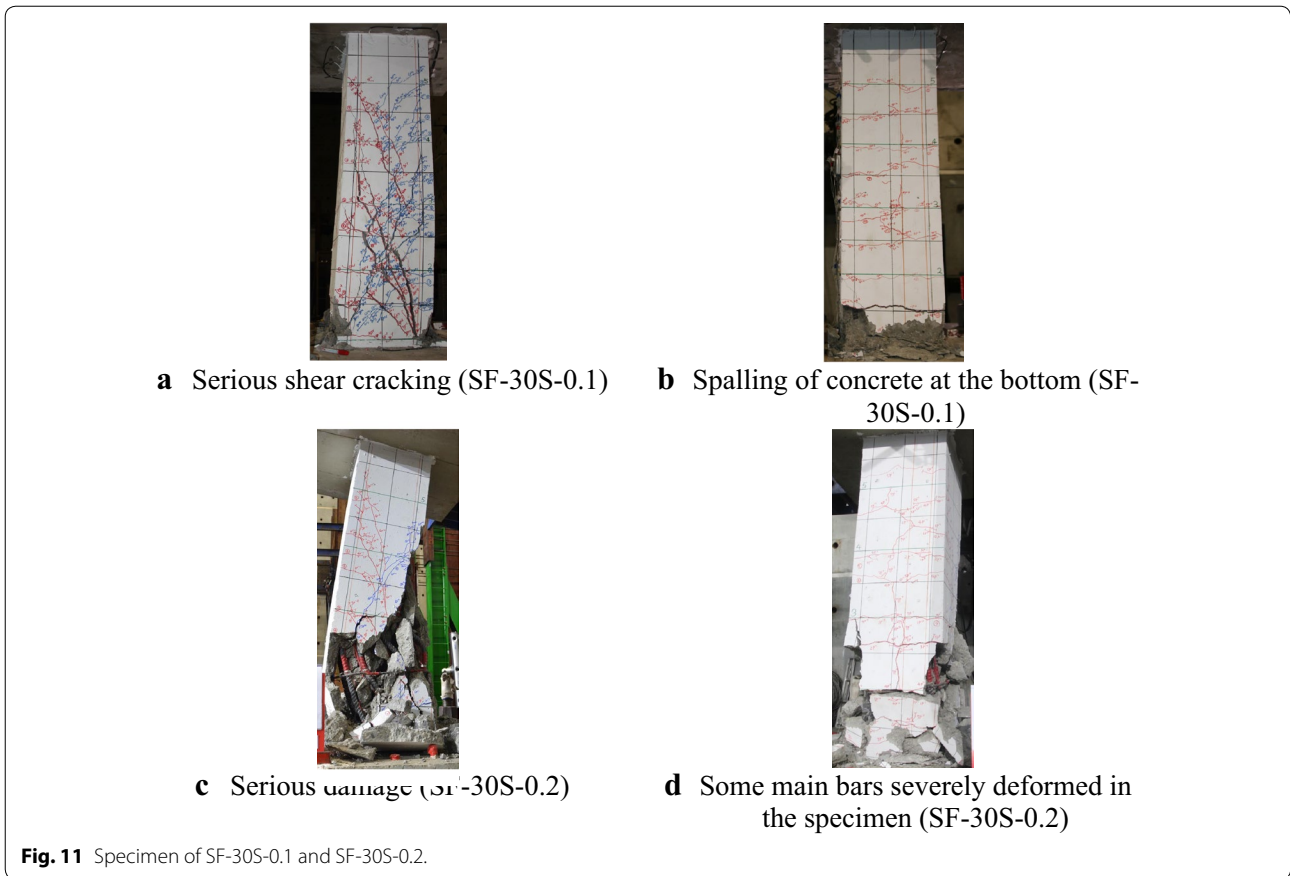
damage level of a column or beam member under seismic loading, as described in Sect. 2.3. According to Fig. 13a, the ratio of residual total shear crack width to residual maximum shear crack width  $n_s$  rises linearly at small shear deformation ( $\leq 0.1\%$ ). Additionally, as shear deformation increases, the ratio  $n_s$  turns to be constant. The literature (AIJ 2004) suggests that the ratio  $n_s$  of an RC column or beam member is 3.0–4.0. The experimental results herein indicate that the mean ratio  $n_s$  of the column specimens is approximately 3.13. Since the standard deviation is 1.08, this work conservatively recommends a required ratio of 2.0 between the residual total shear crack width and residual maximum shear crack width for use in the crack-based damage assessment.

To identify the crack-based performance points on the structural capacity (force–displacement) curve, the ratio of peak total shear crack width to peak maximum shear crack width  $n_{sp}$  and the ratio of the maximum peak shear crack width to the residual maximum crack width  $n_{s,max}$  are also required. This work suggests the ratios  $n_{sp}$  and  $n_{s,max}$  of 2.0 and 1.5, which are the mean value minus one standard deviation, respectively (Fig. 13b, c). This work also investigates the ratio of the residual total flexural crack width to the residual maximum flexural crack width  $n_f$ , the ratio of the peak total flexural crack width to

the peak maximum flexural crack width  $n_{fp}$  and the ratio of the maximum peak shear crack width to the residual maximum crack width  $n_{f,max}$ . Figure 13d–f shows the experimentally determined ratios  $n_f$ ,  $n_{fp}$ , and  $n_{f,max}$ . Based on Fig. 13d–f, this work suggests values of  $n_f$  and  $n_{fp}$  that are determined using the same rule as was used to determine the values of  $n_s$  and  $n_{sp}$ , as shown in Table 7. However, the variation of  $n_{f,max}$  is large and the recommended value of 2.0 is more conservative than the recommended values of other ratios.

#### 4 Reduction Factors of Mechanical Properties of Seismic Capacity

Based on the definition of the damage levels of structural members in Table 1, the maximum residual crack width and damage state that were observed in the experiment can be used to determine the damage level of each specimen. The strength of the specimens clearly decreases at damage level IV. In this work, the lateral force of  $0.8V_{max}$  in the envelope line of hysteretic hoops for a specimen is used to determine the ultimate deformation point as a dividing point between damage levels IV and V. Based on experimental results, this section examines the reduction factors of strength, stiffness and energy dissipation capacity.



Actually, it is not easy to distinguish the flexural failure mode from the flexural–shear failure mode based on the testing results. Generally, for the flexural–shear failure mode of a specimen, when the applied force reaches the shear strength, it can be found that many severe shear cracks occur in the specimen. Additionally, these cracks dominate the deformation capacity of the specimen. This

work also investigates the yielding point of the stirrup in a specimen under the cyclic loading. It can be found that the deformation corresponding to the yielding point of the stirrup is around 3.0–4.0% for the specimens with the flexural failure mode while the yielding point of the stirrup is around 1.5–2.0% for the specimens with the flexural–shear and shear failure modes. Therefore, on

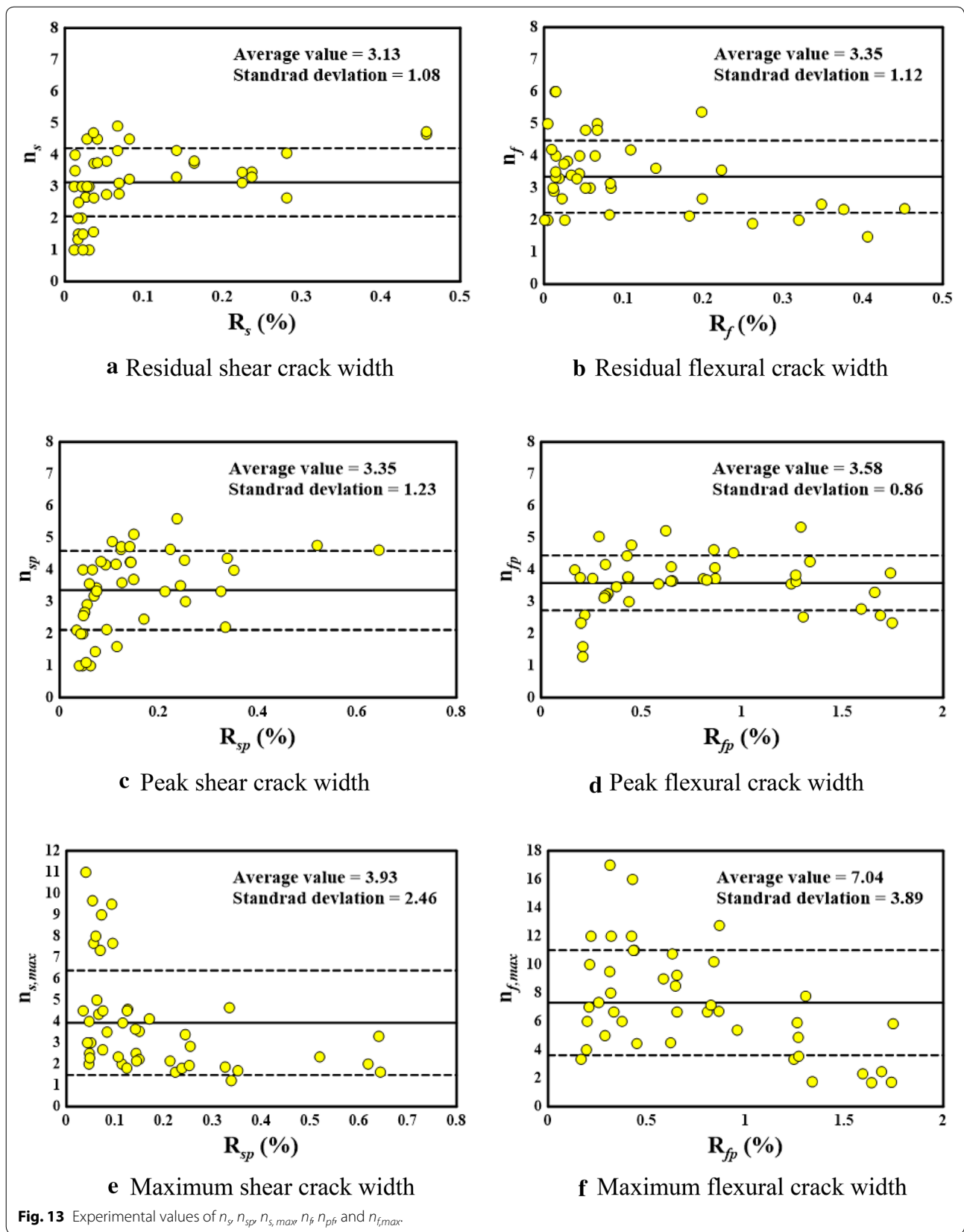


**Table 7 Suggested values of  $n_f$ ,  $n_{sp}$ ,  $n_{s,max}$ ,  $n_p$ ,  $n_{pf}$  and  $n_{f,max}$ .**

Crack types	Suggested values				Reference (AIJ 2004)
Flexural crack	$n_f$	$n_{f,max}$	$n_{fp}$	$n_f$	2
	2	2	2.5	2	
Shear crack	$n_s$	$n_{s,max}$	$n_{sp}$	$n_s$	3–4
	2	1.5	2	3–4	

the basis of the shear crack development and the stress development of the stirrup, this work defines the failure mode for each specimen, as listed in Table 6.

**4.1 Reduction Factor of Energy Dissipation Capacity**

Applying the definition of damage levels of structural members in Table 1, the experimental results herein are utilized to quantify the reduction factors of energy dissipation capacity for RC column members, as described in Sect. 2.1. Figure 14 plots the relationship between the maximum residual flexural crack width and reduction factor of energy dissipation capacity for specimens with flexural and flexural–shear failure modes in the experiment. Figure 14 also plots the reduction factors of energy dissipation capacity at various damage levels and the reduction factors at the damage levels of I, II, III are estimated using the regression lines. Additionally, the reduction factors at the damage level IV are calculated using the dividing point between damage levels of IV and V, which is defined as the ultimate deformation point (Table 8).

Table 9 lists the suggested reduction factors of energy dissipation capacity  $\eta_E$  for each damage level for an RC

**Table 8 Dividing points between the damage levels IV and V.**

Failure mode	Specimen	Drift ratio (%)
Flexural failure	FF-15S-0.1	5.99
		6.03
	FF-15S-0.2	5.86
		6.00
Flexural–shear failure	FSF-15S-0.1	5.66
		6.29
	FSF-15S-0.2	3.93
		3.93
	SF-30S-0.1	3.02
		2.94
Shear failure	SF-30S-0.2	–

column member with various failure modes. For the specimen with the shear failure mode, rather than the maximum residual crack width, the damage state is used to determine the damage level. As suggested in the Japanese guideline (JBDPA 2015), the residual capacity of energy dissipation is assumed to be zero for damage levels IV and V. Since only a few specimens are utilized herein to examine the residual capacity of energy dissipation, this work take conservative reduction factors for RC column members considering the experimental reduction factors and those suggested by the Japanese guideline.

**4.2 Reduction Factor of Strength**

Figure 15 pots the relationship between the maximum residual crack width and lateral force, which is normalized by the maximum lateral force in the experiment.

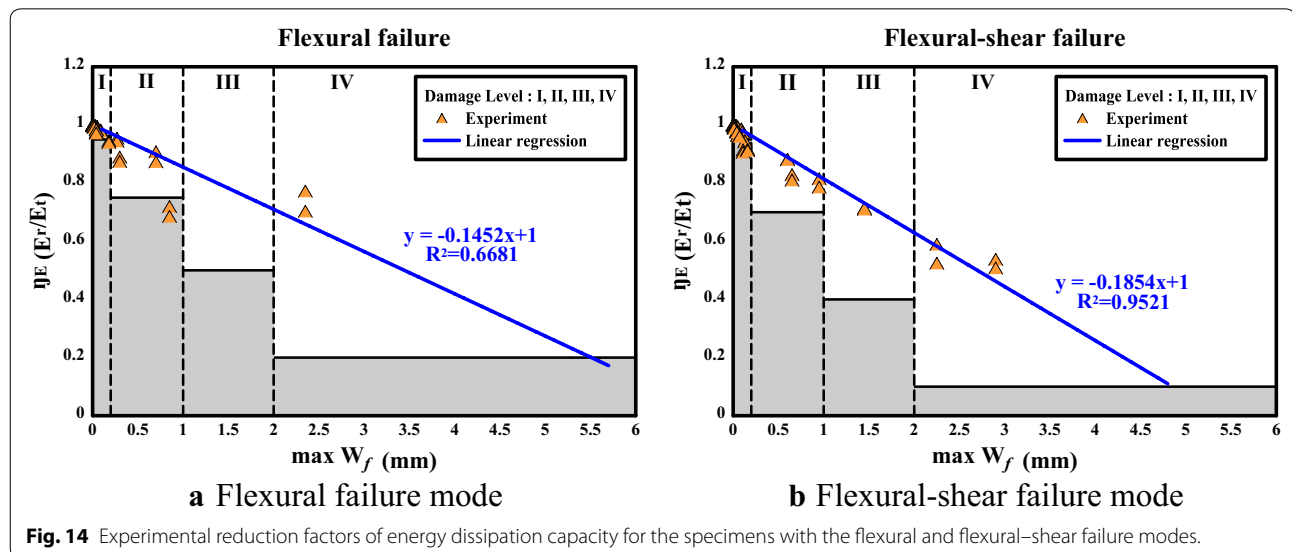


**Fig. 14** Experimental reduction factors of energy dissipation capacity for the specimens with the flexural and flexural–shear failure modes.

**Table 9 Suggested reduction factors of energy dissipation capacity for RC column members.**

Damage level	Suggested values			Reference (JBDPA 2015)		
	Flexural failure	Flexural–shear failure	Shear failure	Flexural failure	Flexural–shear failure	Shear failure
I	0.95	0.95	0.95	0.95	0.95	0.95
II	0.75 (0.85)	0.7 (0.8)	0.6 (0.85)	0.75	0.7	0.6
III	0.5 (0.7)	0.4 (0.6)	0.3 (0.5)	0.5	0.4	0.3
IV	0.1	0.1	0	0.2	0.1	0
V	0	0	0	0	0	0

The value in the parentheses represent experimental reduction factors.

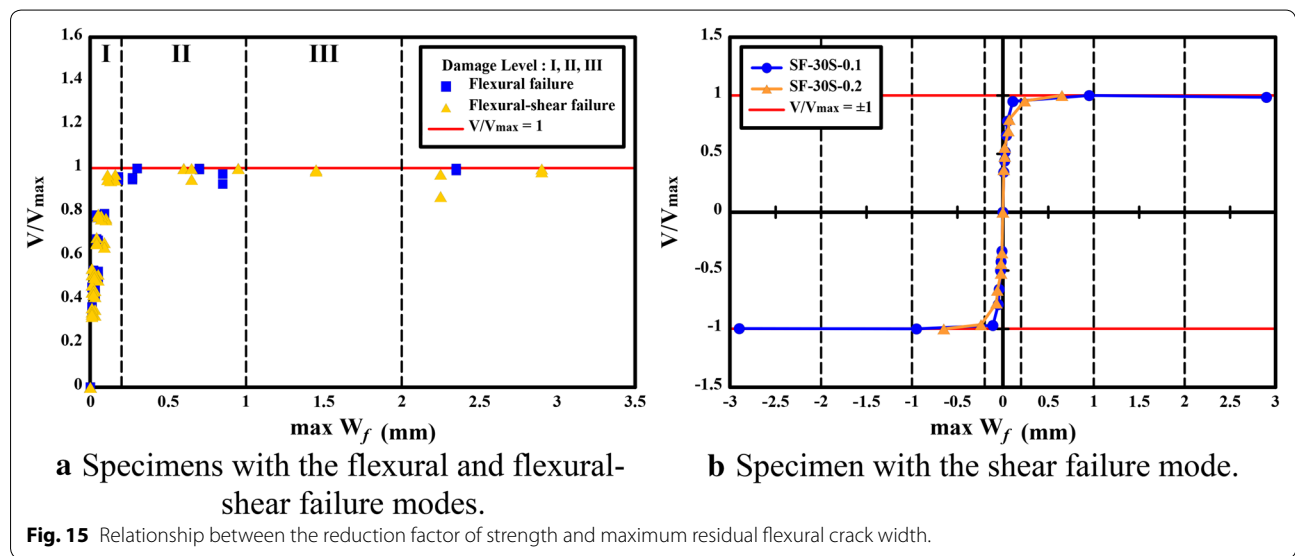


**Fig. 15** Relationship between the reduction factor of strength and maximum residual flexural crack width.

The strength of specimens with flexural and flexural–shear failure modes at damage levels I, II and III can be assumed not to be reduced based on Fig. 15; then, the reduction factors of strength at damage levels I, II, and III can be set to 1.0. Additionally, the reduction factors at the damage level IV are calculated using the dividing point between damage levels of IV and V, i.e., ultimate deformation point.

Table 10 lists the suggested reduction factors of strength  $\eta_V$  at each damage level for an RC column member with various failure modes. The damage state of the specimen with shear failure is used to determine its damage level. Since the maximum lateral force is at the dividing point between damage levels III and IV, the strength falls seriously in damage states IV and V. The residual strength in damage states of IV and V is

**Table 10 Suggested reduction factors of strength for RC column members**

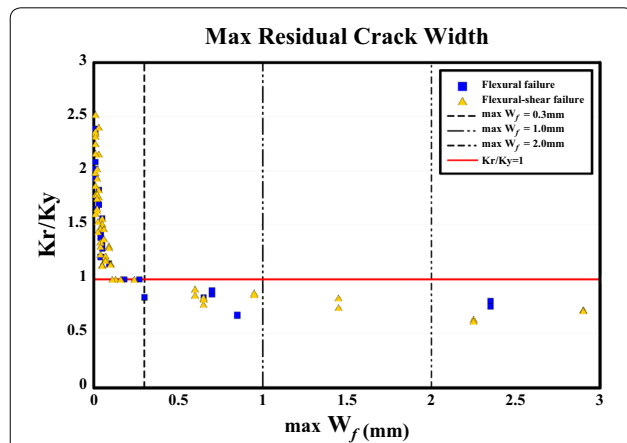
Damage level	Suggested values			Reference (Ito et al. 2015)	
	Flexural failure	Flexural–shear failure	Shear failure	Flexural failure	Shear failure
I	1	1	1	1	1
II	1	1	1	1	1
III	1	1	1	1	1
IV	0.6	0.6 (0.75)	0	0.6	0.4
V	0	0	0	0	0

The value in the parentheses represent experimental reduction factors.

assumed to be zero. As same with the residual capacity of energy dissipation capacity, this work take conservative reduction factors of strength for RC column members considering the experimental reduction factors and those suggested by the Japanese guideline.

### 4.3 Reduction Factor of Stiffness

For the specimens with the flexural and flexural–shear failure modes, Fig. 16 shows the relationship between the maximum residual crack width and residual stiffness (reloading stiffness in the experiment), which is normalized by the original yielding stiffness. According to the definition of damage levels of structural members listed



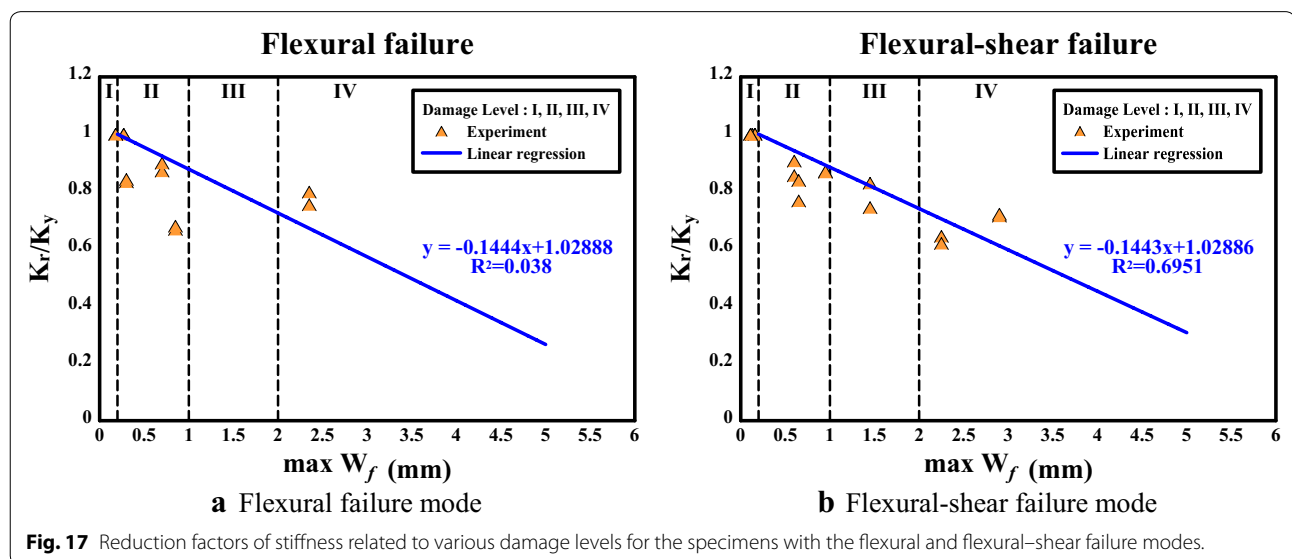
**Fig. 16** Relationship between the maximum residual flexural crack width and residual stiffness for the specimens with the flexural and flexural–shear failure modes.

Table 1, this work uses the experimental results to investigate the reduction factors of stiffness for RC column members. Obviously, in the damage level I, since the specimens are still in the elastic range, the stiffness values are larger than the original yielding stiffness. Therefore, the residual stiffness can be assumed same with the original yielding stiffness (The reduction factor of stiffness is 1.0). Figure 17 shows the experimental reduction factors of stiffness under various damage levels and the reduction factors at the damage levels of I, II, III are estimated using the regression lines. Additionally, the reduction factors at the damage level IV are calculated using the dividing point between damage levels of IV and V, i.e., ultimate deformation point.

For the specimen with the shear failure mode (SF-30S-0.2), instead of the maximum residual crack width, the damage state is used to determine the damage level. Since the maximum lateral force is the dividing point between the damage levels III and IV, the decrease of the stiffness occurs in the damage states of IV and V

**Table 11 Suggested reduction factors of stiffness for RC column members.**

Damage level	Suggested factors		
	Flexural failure	Flexural–shear failure	Shear failure
I	1	1	1
II	0.8	0.8	0.8
III	0.7	0.7	0.7
IV	0.5	0.5	0
V	0	0	0



**Fig. 17** Reduction factors of stiffness related to various damage levels for the specimens with the flexural and flexural–shear failure modes.

obviously. Additionally, in the damage states of IV and V, the stiffness is assumed to be zero. Therefore, this work suggests the reduction factors of stiffness  $\eta_K$ . for each damage level, as listed in Table 11.

## 5 Seismic Performance Assessment Method for RC Buildings

### 5.1 Mechanical Behavior of RC Columns

This work uses the failure model of a column to define the nonlinear plastic hinges of the column (NCREE 2009). This model assumes that the shear strength  $V_n$  degrades with the inelastic deformation beyond the ductility of 2.0. The shear force corresponding to the flexural strength  $V_b$  is assumed constant after the flexural yielding point (Fig. 18);  $V$  is the lateral force and  $\Delta$  is the lateral deformation or displacement). According to the difference between the shear force that corresponds to flexural strength and shear strength, failure modes of a column can be classified as the flexural failure, shear failure, and flexural–shear failure.

Figure 18a shows the flexural failure mode of a column, which occurs when the shear force corresponding to the flexural strength  $V_b$  is less than 60% of the shear strength  $V_n$  (ASCE 2006). In this case, no shear failure exists, and the loading capacity of the member loses due to the fracture of main bars, buckling of main bars or the crush of confined concrete. Figure 18b shows the shear failure mode of a column. This mode occurs when the shear force corresponding to the flexural strength  $V_b$  exceeds the shear strength  $V_n$  (ASCE 2006). In this case, the member is dominated by the shear failure. The column also loses its axial capacity at the axial deformation capacity  $\Delta_a$ .

Figure 18c shows flexure-shear failure mode of a column, which occurs when shear force related to the shear force corresponding to the flexural strength  $V_b$  exceeds  $0.6V_n$  and is less than  $V_n$  (ASCE 2006). In this case, the relationship between the force and deformation of a column is assumed elastic as deformation varies from zero to the yielding deformation  $\Delta_y$  and is constant after the yielding point. Additionally, when the lateral deformation reaches the shear deformation capacity  $\Delta_s$ , shear failure occurs and then the member loses its axial capacity at the axial deformation capacity  $\Delta_a$ . For each performance point of the mechanical behavior in an RC column, i.e., shear drift capacity, axial drift capacity, shear strength and shear force corresponding to flexural strength, can be estimated using Eqs. (5–10), as follows:

#### 5.1.1 Shear Drift Capacity

Based on observations of 50 shear-critical column databases (Elwood and Moehle 2005a), the following empirical Eq. (5) estimates the shear drift capacity of a column with the shear damage:

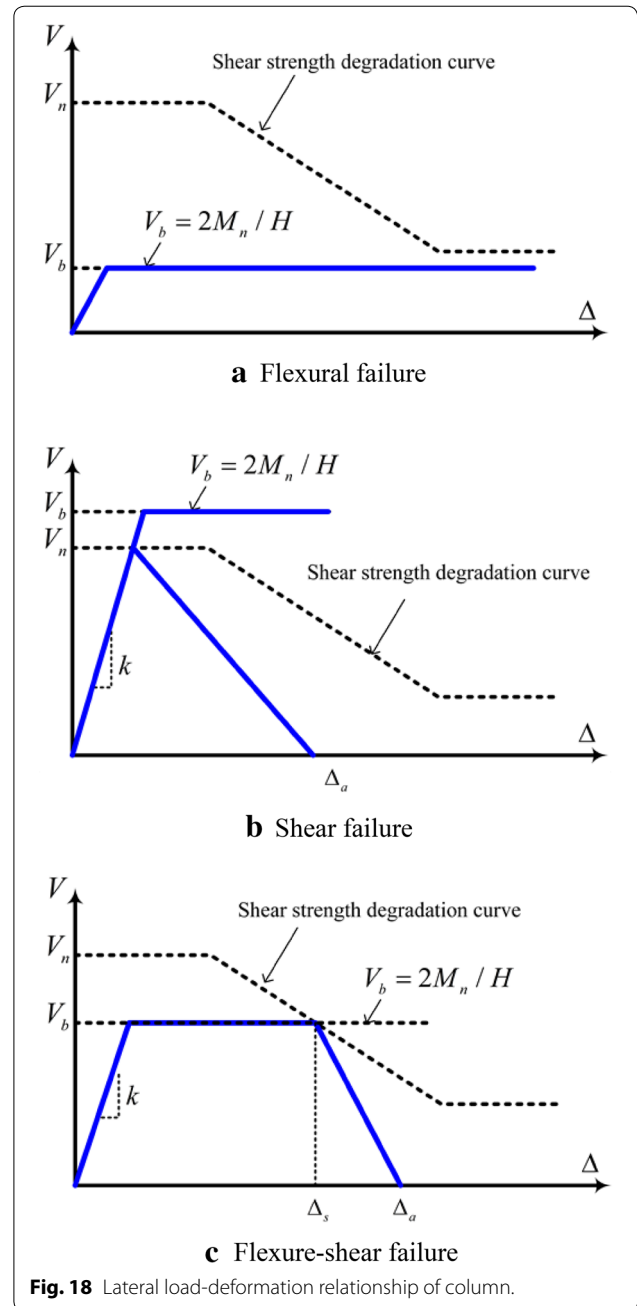


Fig. 18 Lateral load-deformation relationship of column.

$$\frac{\Delta_s}{L} = \frac{3}{100} + 4\rho'' - \frac{1}{133} \frac{v_m}{\sqrt{f'_c}} - \frac{1}{40} \frac{P}{A_g f'_c} \geq \frac{1}{100}, \tag{5}$$

where  $\rho''$  is the transverse reinforcement ratio of  $A_{st}/bs$ ;  $A_{st}$  is the transverse reinforcement area ( $\text{mm}^2$ );  $b$  is the width of a column section ( $\text{mm}$ );  $v_m$  is the maximum shear stress ( $\text{MPa}$ ) as  $V_b/bd$ ;  $d$  is the depth from the extreme fiber of concrete to the centerline of tension reinforcement ( $\text{mm}$ );  $f'_c$  is the compressive strength of

the concrete (MPa);  $P$  is the axial force (N); and  $A_g$  is the gross cross-sectional area of a column ( $\text{mm}^2$ ).

### 5.1.2 Axial drift capacity

In the shear friction model developed by Elwood and Moehle (2005b) to estimate the axial drift capacity of a column with the shear damage, the axial drift capacity is a function of the axial load, amount of transverse reinforcement and critical angle, as shown in Eq. (6).

$$\frac{\Delta_a}{L} = \frac{4}{100} \frac{1 + (\tan\theta)^2}{\tan\theta + P \frac{s}{\kappa' A_{st} f_{yt} d_c \tan\theta}}, \quad (6)$$

where  $f_{yt}$  is the yield strength of transverse reinforcement (MPa);  $d_c$  is the depth of the column core from the centerline to the centerline of the ties (mm), and  $\kappa'$  is the modification factor based on the effect of the hook angle. The critical angle  $\theta$  is the angle between the shear failure plane of a column and the horizontal direction; this angle is approximately  $65^\circ$  or  $\theta = 55 + 35P/P_o$  ( $P_o$  is the axial capacity of an undamaged column and  $P$  is the axial force).

### 5.1.3 Shear Strength

According to ACI 318-05 (2005), the shear strength of a column depends on the contributing effects of the concrete  $V_c$  and transverse reinforcement  $V_s$ , and can be estimated as follows:

$$V_n = V_c + V_s \quad (7)$$

$$V_c = 0.5 \left( 1 + \frac{P}{140A_g} \right) \sqrt{f'_c} bd \quad (8)$$

$$V_s = \frac{A_{st} f_{yt} d}{s} \quad (9)$$

### 5.1.4 Shear Force Related to Flexural Strength

Since beam members in low-rise RC buildings are often constructed with slabs (as T-beams), low-rise buildings behave like shear buildings. Therefore, this work assumes the column deforms in double curvature. The shear force related to flexural strength is the lateral load required to reach the flexural strength  $M_n$  at the column end and the flexural shear strength of a column with the double curvature can be calculated as follow:

$$V_b = \frac{2M_n}{L} \quad (10)$$

## 5.2 Assessment of Seismic Performance

Seo et al. (2015) selected a twelve-story reinforced concrete moment-resisting frame structure with shear walls to

generate a 3D finite element models and evaluate seismic performance using response spectrum analysis and non-linear time-history analysis approaches on the structure. Beside this, the seismic fragility curves for each floor of the structure were generated to evaluate seismic vulnerability of the structure. Additionally, Mushtaq et al. (2018) take 2D and 3D models of multilayer RC buildings as a case study, and the static cyclic analysis was performed and seismic vulnerability assessment was carried out using the capacity spectrum method. They also concluded that the 3D model is more brittle, cracked earlier, and more susceptible to earthquakes than 2D counterparts. Therefore, this work adopts the 3D model of a multilayer RC building and pushover analysis to simulate its capacity curve, which is the relationship between base shear force  $V_{Base}$  and roof displacement  $\Delta_R$ . Additionally, according to the ATC-40 (1996), a constant gravity load combining dead and live loads should be considered in the pushover analysis. The capacity curve is converted to the capacity spectrum, which represents structural performance of the SDOF system for a building by identifying the dynamic characteristics of a structure in terms of the first modal participation factor and the first modal mass coefficient. The ATC-40 (1996) defines the inelastic response of the SDOF system for a building during an earthquake, i.e., acceleration and displacement, as the intersection between its capacity spectrum and its design response spectrum. However, iterative calculations are often needed to find the intersection point. Instead of iterative calculations (NCREC 2009), the capacity spectrum can be transformed into a seismic performance curve according to the design response spectrum modified by the equivalent damping ratio  $\xi_{eq}$  and equivalent fundamental period  $T_{eq}$  (secant period). The curve can then be used to determine the relationship between performance-based ground acceleration and response spectral displacement.

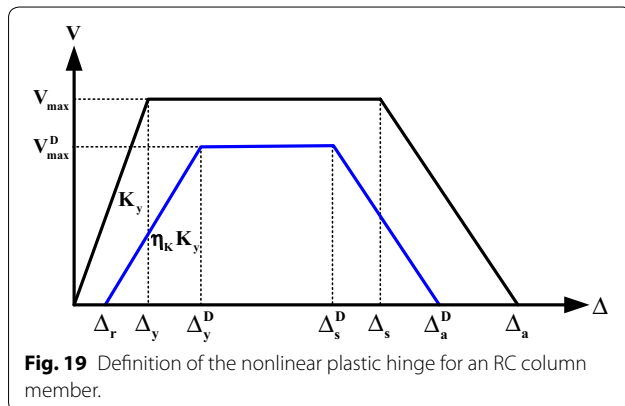
This work defines the ultimate state of an RC building according to the maximum base shear force and the drift ratio of 2.0% (NCREC 2009). The performance point on the capacity spectrum corresponding to the specified ultimate state can be derived as  $(S_{dp}, S_{ap})$ . Accordingly, the response spectral displacement for the specified performance is the same as the ultimate deformation of the SDOF system for a building, i.e.,  $S_{dp} = \delta_u$ . This work uses Eq. (11) to estimate the performance-based ground acceleration corresponding to ultimate deformation of the SDOF system for a building  $A_p$ .

$$A_p = \left\{ \begin{array}{l} \left[ \frac{S_{ap}}{1 + \left( \frac{2.5}{B_s} \right) \frac{T_{eq}}{0.2T_o}} \right], \quad \text{for } T_{eq} \leq 0.2T_o \\ \frac{B_s}{2.5} S_{ap}, \quad \text{for } 0.2T_o \leq T_{eq} \leq T_o \\ \frac{B_s T_{eq}}{2.5 T_o} S_{ap}, \quad \text{for } T_o \leq T_{eq} \end{array} \right\}, \quad (11)$$

where  $S_{ap}$ ,  $T_o$ ,  $B_s$  and  $T_{eq}$  are the spectral acceleration (g) for the peak effective inelastic limit, the boundary period between the short-period range and the medium-period range, the modification factor of the damping ratio in terms of the equivalent damping ratio  $\xi_{eq}$  and the equivalent fundamental period ( $=2\pi\sqrt{S_{dp}/(S_{ap} \times g)}$ ), respectively.

### 5.3 Definition of Nonlinear Plastic Hinges for Damaged RC Column Members

In order to define the nonlinear plastic hinges of damaged RC column members in the pushover analysis, the mechanical properties of damaged RC column members should be evaluated considering the residual strength, residual stiffness and residual capacity of energy dissipation. For an RC column member with a specified damage state, its residual strength  $V_{max}^D$  and residual stiffness  $K_y^D$  can be evaluated using Eqs. (12) and (13) ( $K_y (=0.35 \left(\frac{12E_c I_g}{L^3}\right))$  is the yielding stiffness of an RC member without any damage); NCREE (2009). Additionally, when a perfect elastic–plastic mechanical model (Fig. 19) is used to define the capacity of energy dissipation for an RC column member, the reduction factor of energy dissipation capacity can be calculated using Eq. (14). In Eq. (14), the residual deformation  $\Delta_r$  can be obtained using the maximum residual flexural crack width related to a specified damage level. On the basis of Eqs. (12) and (13), the yielding displacement of an RC column member with a specified damage level  $\Delta_y^D$  can be estimated using Eq. (15); furthermore, by substituting Eq. (15) into Eq. (14), its corresponding shear deformation capacity  $\Delta_s^D$  can be estimated using Eq. (16). After the point of the shear deformation capacity for an RC column member with a specified damage  $\Delta_s^D$ , this work assumes the slope of stiffness degradation does not change and then the axial deformation capacity  $\Delta_a^D$  can be obtained using Eq. (17). Then, Eqs. (12, 13, 14) and (15) can be used to define the nonlinear plastic hinge for an RC column member with a specified damage.



$$V_{max}^D = \eta_V \times (V_n \text{ or } V_b) \tag{12}$$

$$K_y^D = \eta_K \times K_y \tag{13}$$

$$\eta_E = \frac{E_r}{E_t} = \frac{(2\Delta_s^D - \Delta_y^D - \Delta_r)}{(2\Delta_s - \Delta_y)} \times \eta_V \tag{14}$$

$$\Delta_y^D = \left(\frac{\eta_V}{\eta_K}\right) \Delta_y + \Delta_r \tag{15}$$

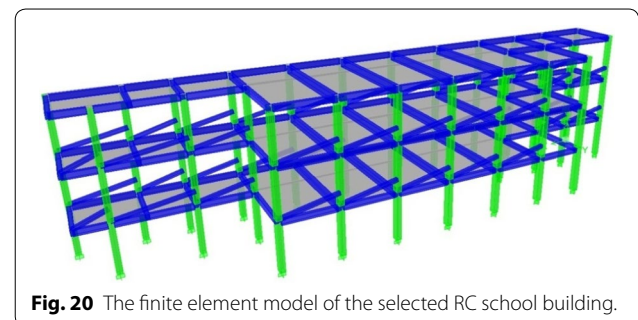
$$\Delta_s^D = \left(\frac{\eta_E}{\eta_V}\right) \Delta_s + \left(\frac{\eta_V}{2\eta_K} - \frac{\eta_E}{2\eta_V}\right) \Delta_y + \Delta_r \tag{16}$$

$$\Delta_a^D = \frac{V_{max}^D}{V_b} (\Delta_a - \Delta_s) + \Delta_s^D \tag{17}$$

Generally, the residual deformation  $\Delta_r$  cannot be considered in the pushover analysis. Therefore, the residual deformation  $\Delta_r$  is set at zero in the definition of the nonlinear plastic hinge. Additionally, for a member with the flexural or flexural–shear failure, if the shear deformation capacity  $\Delta_s^D$  is smaller than the yielding deformation  $\Delta_y^D$ , it means that its failure mode would change to the shear failure, as shown in Fig. 19.

### 5.4 Case Study

Figure 20 shows the finite element model built in the ETABS (CSI 2008) for an RC school building selected for a case study. Their detailed information can be found in the reference (NCREE 2012). The damage level of each vertical component of these buildings was determined according to visual inspections of these buildings and damage classifications (Table 1). For the selected building, damaged components were on the first floor (Fig. 21). Four columns were damaged most with flaking concrete covers and no crushing on their concrete cores; therefore, they were classified as damage level IV



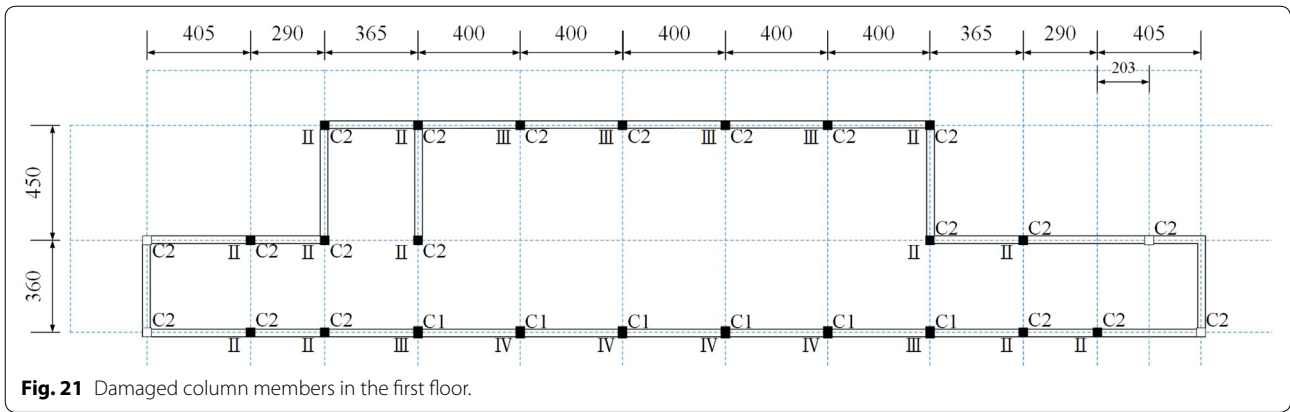


**Fig. 21** Damaged column members in the first floor.



**a** Damage Level IV      **b** Damage Level III  
**Fig. 22** Damage levels of damaged column members.

	C1	C2	C3
Cross Section			
Main Bar	12-#8	12-#8	12-#8
Hoop Bar (mm)	#3@300	#3@250	#3@250
B × D (mm)	350 × 450	350 × 450	350 × 350

Note:  
 Average compression strength of concrete is 15.0 MPa.  
 Yielding strength of reinforcing steel is 280 MPa.

**Fig. 23** Detailed information needed in the pushover analysis.

(Fig. 22a). Additionally, Fig. 22b shows a column with flaking tile and brick, which was classified as damage level III.

According to the literature (NCREC 2009), infill walls are an efficient way to upgrade the seismic performance of an RC building. In Taiwan, low-rise RC buildings often lack infill walls in the longitudinal direction, which is generally parallel with the corridors. Because of the lack of infill walls, low-rise RC buildings have lower seismic performance in the longitudinal direction than the other direction. Therefore, this case study only assessed the seismic performance of the longitudinal direction for the selected buildings. Figure 23 shows the detailed columns for the pushover analysis. Besides the nonlinear hinge setting described in Sect. 5.1, the pushover analysis assumes a rigid diaphragm in the finite element models. The pushover analysis should be applied to acquire the capacity curves before and after the earthquake (Fig. 24). The seismic capacity before and after the earthquake can be obtained according to the capacity curves and the detailed seismic performance assessment (Table 12). The seismic residual ratios determined using the detailed

seismic performance assessment method. Additionally, the peak ground acceleration of earthquake-damaged seismic capacity for the selected building  $D A_p$  is indeed smaller than the code-required performance  $A_T$  (Table 12). Therefore, all three buildings require the seismic retrofit.

### 6 Conclusions

This work provided reduction factors of seismic capacity for RC columns with various failure modes based on experimental data and the past researches. For an RC column member with seismic damage, besides of the energy dissipation capacity, the residual strength and residual stiffness can be quantified using the suggested reduction factors summarized in Table 13 in this work. According to the damage states of RC columns and their corresponding reduction factors suggested herein, this work proposes the seismic performance assessment method for the residual seismic performance of earthquake-damaged low-rise RC buildings. This work selected one building damaged in the earthquake to

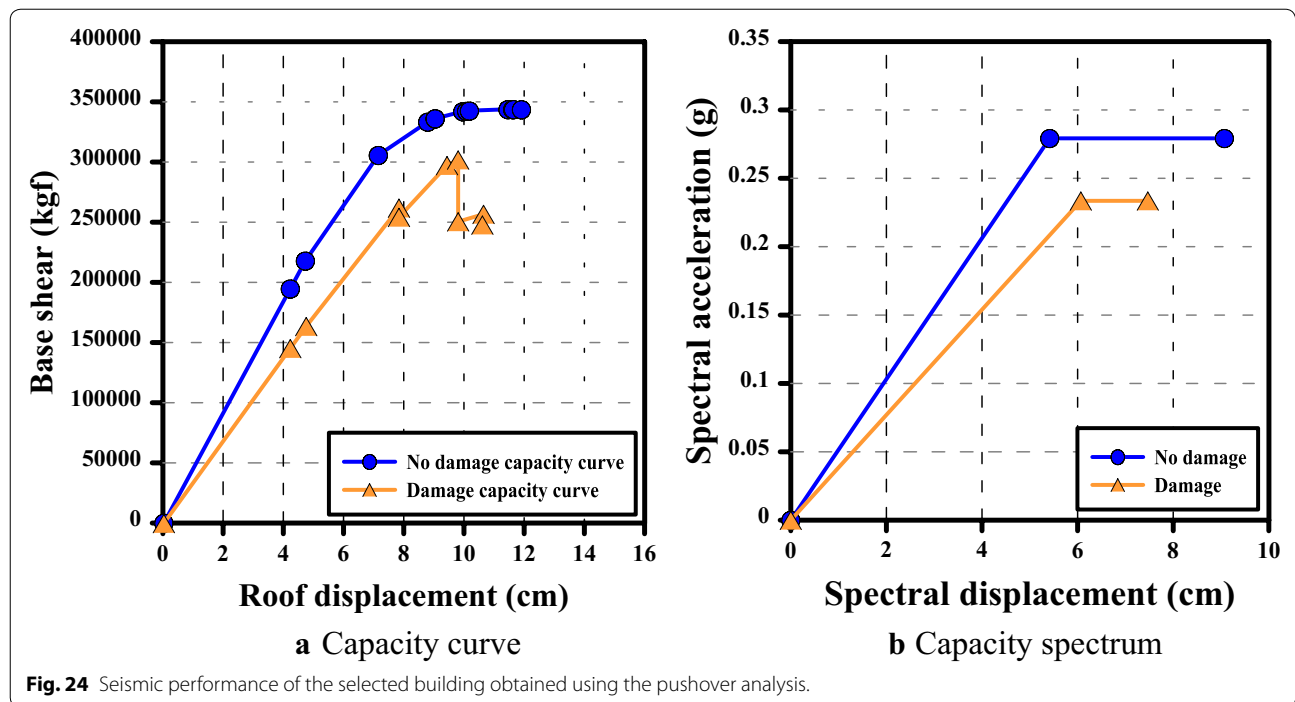


**Table 12 Residual performance of seismic capacity.**

Mechanical properties	Before earthquake	After earthquake	Reduction ratio
Strength (kgf)	343,851	302,061	87.9%
Stiffness (kgf/cm)	42,724	33,417	74.7%
Performance-based ground acceleration (g), $A_p$	0.199	0.145 <sup>a</sup>	72.7%
Code-required ground acceleration (g) (MOI 2005), $A_T$			0.308

<sup>a</sup>  $A_p$ : Peak ground acceleration of earthquake-damaged seismic capacity.

**Table 13 Suggested reduction factors of energy dissipation capacity, strength and stiffness for RC column members.**

Damage level	Flexural failure			Flexural–shear failure			Shear failure		
	$\eta_E$	$\eta_V$	$\eta_K$	$\eta_E$	$\eta_V$	$\eta_K$	$\eta_E$	$\eta_V$	$\eta_K$
I	0.95	1	1	0.95	1	1	0.95	1	1
II	0.75	1	0.8	0.7	1	0.8	0.6	1	0.8
III	0.5	1	0.7	0.4	1	0.7	0.3	1	0.7
IV	0.1	0.6	0.5	0.1	0.6	0.5	0	0	0
V	0	0	0	0	0	0	0	0	0

demonstrate the post-earthquake assessment of seismic performance. In the future, when many buildings are damaged by a large earthquake, a post-earthquake emergent decision-making procedure for damaged low-rise RC buildings can be conducted using the proposed residual seismic performance assessment method and

then determine the strategies for the damaged buildings. However, this work only suggests the reduction factor of damaged column components. Other structural components (such as beam-column joints and walls) will also affect the post-earthquake residual seismic performance of structures in the pushover analysis,

and it requires further researches to consider the effects of other components.

#### Authors' contribution

C-KC proposed the main structure of this research and concluded the proposed models in this research. H-FS and K-NC conducted the experiment and analysis. F-PH provided the suggestions in the nonlinear static analysis in the case study. All authors read and approved the final manuscript.

#### Competing interests

The authors declare that they have no competing interests.

Received: 28 September 2017 Accepted: 5 February 2019

Published online: 07 October 2019

#### References

- ACI Committee (American Concrete Institute). (2005). *Building code requirement for structural concrete (ACI 318-05) and commentary (318R-05)*. Michigan, USA: Farmington Hills.
- AIJ (Architecture Institute of Japan). (2004). *Guidelines for performance evaluation of earthquake resistant reinforced concrete buildings (Draft)*. Japan: Tokyo.
- ASCE (American Society of Civil Engineers). (2006). *Seismic rehabilitation of existing buildings (ASEC-41)*. Virginia, USA: Reston.
- ATC (Applied Technology Council). (1996). *Seismic evaluation and retrofit of concrete buildings (ATC-40)*. California, USA: Redwood City.
- CSI (Computer and Structures, Inc.). (2008). *Extended 3D analysis of building systems (ETABS), nonlinear version 9.5*. Berkeley, California, USA: User's Manual.
- Di Ludovico, M., Polese, M., d'Aragona, M. G., Prota, A., & Manfredi, G. (2013). A proposal for plastic hinges modification factors for damaged RC columns. *Engineering Structures*, 51, 99–112.
- Elwood, K. J., & Moehle, J. P. (2005a). Drift capacity of reinforced concrete columns with light transverse reinforcement. *Earthquake Spectra*, 21(1), 71–89.
- Elwood, K. J., & Moehle, J. P. (2005b). Axial capacity model for shear-damaged columns. *ACI Structural Journal*, 102(4), 578–587.
- FEMA (Federal Emergency Management Agency). (1998). *NEHRP guidelines for the seismic rehabilitation of buildings (FEMA-273)*. Washington, D.C.: FEMA.
- FEMA (Federal Emergency Management Agency). (2000). *Prestandard and commentary for the seismic rehabilitation of buildings (FEMA-356)*. Washington, D.C.: FEMA.
- Ito, Y., Suzuki, Y., & Maeda, M. (2015). Residual seismic performance assessment for damaged RC building considering the reduction of strength, deformation and damping ratio. *Proceeding of JCI Annual Convention (Japan Concrete Institute)*, 37(2), 787–792.
- JBDPA (Japan Building Disaster Prevention Association). (2001). *Guideline for post-earthquake damage evaluation and rehabilitation*. Tokyo, Japan: JBDPA.
- JBDPA (Japan Building Disaster Prevention Association). (2015). *Standard for seismic evaluation of existing reinforced concrete buildings, guidelines for seismic retrofit of existing reinforced concrete buildings, and technical manual for seismic evaluation and seismic retrofit of existing reinforced concrete buildings*. Tokyo, Japan: JBDPA.
- MOI (Minister of the Interior of Taiwan). (2005). *Seismic design code for buildings*. Taipei, Taiwan: MOI.
- Mushtaq, A., Khan, S. A., Ahmad, J., & Ali, M. U. (2018). Effect of 3D models on seismic vulnerability assessment of deficient RC frame structures. *Australian Journal of Structural Engineering*, 19(3), 214–221.
- NCREC (National Center for Research on Earthquake Engineering of Taiwan). (2009). *Technology handbook for seismic evaluation and retrofit of school buildings (NCREC-09-023)*. Taipei, Taiwan: NCREC.
- NCREC (National Center for Research on Earthquake Engineering of Taiwan). (2012). *Seismic performance evaluation deteriorating and earthquake-damaged RC school buildings (NCREC-12-018)*. Taipei, Taiwan: NCREC.
- Park, Y. J., & Ang, A. H.-S. (1985). Mechanistic seismic damage model for reinforced concrete. *Journal of the Structural Engineering (ASCE)*, 111(4), 722–739.
- Poegoeh, A. C. (2012). *Reduction factors of seismic capacity for earthquake-damaged reinforced concrete columns*. Master thesis, National Taiwan University of Science and Technology.
- Seo, J., Hu, J. W., & Davaajamts, B. (2015). Seismic performance evaluation of multistory reinforced concrete moment resisting frame structure with shear walls. *Sustainability*, 7, 14287–14308.
- Sugi, T., Ishimori, A., Tajima, K., & Shirai, N. (2007). Damage evaluation of RC beam members based on accurate measurement of displacement and crack widths with scanner (Part 2): Proposal of rational suggestion of quantitative evaluation model for evaluating of shear crack width-shear deformation relationship, *Summaries of Technical Papers of Annual Meeting of Architectural Institute of Japan (AIJ)*, C-2, 373–374.

#### Publisher's Note

Springer Nature remains neutral with regard to jurisdictional claims in published maps and institutional affiliations.

Submit your manuscript to a SpringerOpen® journal and benefit from:

- Convenient online submission
- Rigorous peer review
- Open access: articles freely available online
- High visibility within the field
- Retaining the copyright to your article

Submit your next manuscript at ► [springeropen.com](https://www.springeropen.com)